Optimal Meter Placement in Low Observability Distribution Networks with DER

Diogo M.V.P. Ferreira, Pedro M.S. Carvalho and Luís A.F.M. Ferreira
Department of Electrical and Computer Engineering
IST and INESC-ID
Lisbon, Portugal
{diogomvpferreira, pcarvalho, lmf}@tecnico.ulisboa.pt

***Abstract*—This paper presents a mixed integer linear programming (MILP) approach to deal with the volatility associated with loads and distributed energy resources (DER) in low observability distribution networks. Distribution networks, characterized by having many buses and few meters, have recently faced massive integration of DER, whose injection increases net load volatility. To better understand how to act under such increased volatility, the accuracy of state estimation (SE) needs to be improved. Our approach improves SE accuracy by providing meter placement solutions that take into account uncertainty as expressed by multiple load and DER profile scenarios, this way mitigating the impact of net load volatility. Solution results are illustrated and discussed for different case studies carried out over a radial 9 bus test feeder.**

***Index Terms*—Distribution networks, limited observability, load and DER volatility, MILP, optimal meter placement**

I. Introduction

In recent years, the European Union (EU) has been promoting policies towards reducing greenhouse gas emissions around 80-95% by 2050, as part of the Energy Roadmap 2050 [1]. To accomplish this objective, the EU set the goal of 20% of integration of renewable energy sources by 2020 [2] and, more recently, established a binding target of a share of at least 32% by 2030 [3]. This process of decarbonization of the energy sector is expected to occur mainly at the distribution level, contributing to the expansion of DER and placing pressure in a system that was designed with a static mindset [2], [4]. Besides this, the volatile nature of loads and the large extension of distribution networks compromise the efficient monitoring of the network. Consequently, distribution system operators need to adapt to this new situation to secure their services [2], [5]. Inevitably, it is required a more precise knowledge of the state in distribution networks. However, obtaining greater accuracy in SE becomes challenging as the available information is mostly obtained from pseudo-measurements, measurements with high variance [6]. In addition, placing a large number of meters in the network is economically unsustainable. Under these conditions, the meter placement problem needs to be solved considering volatile loads and DER, low observability and a restricted budget.

The meter placement problem was introduced by Schweppe and Wildes [7]. In their seminal paper, the importance of the covariance matrix of the state estimate was highlighted for both SE and its possible use in the allocation of new measurements. Later on, Monticelli and Wu [8] proposed a meter placement algorithm whose objective was to achieve observability in the network. This algorithm started by identifying the observable parts of the network, called observable islands, through the factorization of the gain matrix. Afterwards, pseudo-measurements were used in order to merge all observable islands into one.

More recently, new approaches have been proposed and were mainly focused on distribution networks. Singh, Pal and Vinter [9] aimed to decrease the relative errors in the voltage and angle estimates at all buses of the network, which was derived to be equivalent to reducing the error ellipse generated by the covariance matrix of the state estimate. Chen et al. [10] used a circuit representation model based on the gain matrix to represent SE errors and a disjunctive model to exactly relax and convert the meter placement problem from a mixed integer nonlinear programming (MINLP) problem into a MILP problem. Furthermore, some papers focused on addressing the meter placement problem in active distribution networks [11], [12]. These approaches relied on the use of heuristics to obtain the desired meter placement solution, specifically a genetic algorithm and a binary particle swarm optimization method.

This paper addresses the meter placement problem in distribution networks under low observability, mitigating the impact of load and DER volatility in meter placement solutions. The objective is to attain maximum accuracy in SE by providing a compromise solution that prevents a significant increase in SE errors. For this reason, the original MILP formulation by Chen et al. [10] was extended so as to deal with the uncertainty expressed by multiple scenarios of different load and DER profiles. Each of these scenarios corresponds to the set of power measurements obtained at each bus under a determined time interval. Furthermore, each meter placement solution comprises the allocation of a limited number of meters, voltage magnitude measurements and/or current magnitude measurements, with high accuracy.

This paper is organized as follows. Section II presents the SE theory applied to this work and details the steps towards the formulation of the MILP approach. Section III describes the case study and the tests performed. In Section IV analysis are drawn on the results obtained from the tests performed. Finally, Section V summarizes the main conclusions of the work.

II. Proposed Approach

A. State Estimator

The state estimator considered in this approach is the weighted least squares based on an AC network model. Hence, the relation between the state variables and the measurements can be defined as

$$\boldsymbol{z} = \boldsymbol{h}(\boldsymbol{x}) + \boldsymbol{e} \tag{1}$$

where $\boldsymbol{z}$ is the measurement vector (m-vector); $\boldsymbol{x}$ is the state vector (n-vector); $\boldsymbol{h}(.)$ is the measurement function, which is a nonlinear vector function that relates measurements to states (m-vector) and $\boldsymbol{e}$ is the the measurement error vector (m-vector) [13], [14]. The measurement error considered has zero mean, and the errors are assumed independent. From these properties, the measurement error covariance matrix is formulated as a diagonal matrix, where each diagonal element is the variance associated with each measurement allocated.

$$Cov(\boldsymbol{e}) = E[\boldsymbol{e}\boldsymbol{e}^T] = \boldsymbol{R_z} = diag\{\sigma_1^2, \sigma_2^2, \ldots, \sigma_m^2\} \tag{2}$$

Furthermore, once measurement errors are considered random variables, the same assumption can be extended to the measurements $\boldsymbol{z}$. These variables can also be represented according to a Gaussian distribution with a covariance matrix identical to (2), but with mean $\boldsymbol{h}(\boldsymbol{x})$ [15].

To obtain the maximum likelihood estimate, the objective function $J(\boldsymbol{x})$

$$J(\boldsymbol{x}) = \left[\boldsymbol{z} - \boldsymbol{h}(\boldsymbol{x})\right]^T \boldsymbol{R_z}^{-1} \left[\boldsymbol{z} - \boldsymbol{h}(\boldsymbol{x})\right] \tag{3}$$

is minimized

$$\min_{\boldsymbol{x}} J(\boldsymbol{x}) \tag{4}$$

The first-order optimal condition of (4) is given by

$$\boldsymbol{g}(\boldsymbol{x}) = \frac{\partial J(\boldsymbol{x})}{\partial \boldsymbol{x}} = 0 \Leftrightarrow -\boldsymbol{H}^T(\boldsymbol{x})\boldsymbol{R_z}^{-1}\left[\boldsymbol{z} - \boldsymbol{h}(\boldsymbol{x})\right] = 0 \tag{5}$$

where $\boldsymbol{g}(\boldsymbol{x})$ is the gradient of $J(\boldsymbol{x})$ and $\boldsymbol{H}(\boldsymbol{x})$ is the Jacobian matrix of the measurement function

$$\boldsymbol{H}(\boldsymbol{x}) = \frac{\partial \boldsymbol{h}(\boldsymbol{x})}{\partial \boldsymbol{x}} \tag{6}$$

The gradient obtained in (5) is a nonlinear function and, consequently, in order to obtain a solution it is necessary to use an iterative method. For this reason, Newton's method is used to solve $\boldsymbol{g}(\boldsymbol{x}) = 0$. After applying the Taylor expansion to $\boldsymbol{g}(\boldsymbol{x})$,

$$\boldsymbol{g}(\boldsymbol{x}) = \boldsymbol{g}(\boldsymbol{x}^k) + \boldsymbol{G}(\boldsymbol{x})(\boldsymbol{x} - \boldsymbol{x}^k) + \cdots = 0 \tag{7}$$

where $\boldsymbol{G}(\boldsymbol{x})$ is referred to as the gain matrix. This Hessian matrix of the objective function can be expressed as

$$\boldsymbol{G}(\boldsymbol{x}) = \frac{\partial^2 J(\boldsymbol{x})}{\partial \boldsymbol{x}^2} = \boldsymbol{H}^T(\boldsymbol{x})\boldsymbol{R_z}^{-1}\boldsymbol{H}(\boldsymbol{x}) \tag{8}$$

after ignoring the second derivative terms. Finally, after disregarding higher order terms of (7) and using (5), an iterative solution can be found

$$\begin{aligned} \boldsymbol{G}(\boldsymbol{x})\Delta\boldsymbol{x}^k &= \boldsymbol{H}^T(\boldsymbol{x})\boldsymbol{R_z}^{-1}\left[\boldsymbol{z} - \boldsymbol{h}(\boldsymbol{x})\right] \\ \Delta\boldsymbol{x}^k &= \boldsymbol{x}^{k+1} - \boldsymbol{x}^k \end{aligned} \tag{9}$$

to solve SE [13]–[15].

B. Circuit Representation of the Gain Matrix

The gain matrix is a key element in meter placement. It reflects both the type, accuracy and location of the measurements placed in a system. In addition, according to Schweppe and Wildes [7] its inverse matrix

$$\boldsymbol{R_{\hat{x}}} = \boldsymbol{G}^{-1} \tag{10}$$

can be interpreted as a measure of accuracy of the state estimate

$$\boldsymbol{R_{\hat{x}}} = E\{(\boldsymbol{x} - \hat{\boldsymbol{x}})(\boldsymbol{x} - \hat{\boldsymbol{x}})^T\} \tag{11}$$

Accordingly, $\boldsymbol{R_{\hat{x}}} = (\varepsilon_{ij})_{n\times n}$ can be referred to as the covariance matrix of the state estimate, as it provides information about the accuracy which can be achieved at each bus with the available measurements.

Furthermore, the gain matrix is a symmetric sparse matrix. Consequently, its structure is similar to the admittance matrix $\boldsymbol{Y}$, which is characterized for its use to describe networks in power systems. Chen et al. [10] used this fact to represent SE errors through a circuit representation model of the gain matrix

$$\boldsymbol{G} = \sum_{k=1}^{N_b} \boldsymbol{M}_k y_k \boldsymbol{M}_k^T \tag{12}$$

where $\boldsymbol{M}_k$ is a vector that represents the location of each admittance y_k, and N_b is the number of branches. The reasoning used to obtain the admittances from matrix $\boldsymbol{Y}$ is also used for the gain matrix

$$\begin{cases} y_i^{SA} = \sum\limits_{j=1}^{n} G_{ij} \\ y_{ij}^{BA} = -G_{ij} \end{cases} \tag{13}$$

where y_i^{SA} is the shunt admittance of bus i and y_{ij}^{BA} is the branch admittance between buses i and j.

The only remaining issue to complete the circuit representation is to know how to compute the elements of the gain matrix. For this reason, (8) can be used in a summation form expressed as

$$G_{ij} = \sum_{k=1}^{m} \frac{h_{ki}h_{kj}}{\sigma_k^2} \tag{14}$$

where k is the measurement index; i, j are the indices of each element of the gain matrix and h_{ki} and h_{kj} are the individual elements of $\boldsymbol{H}$, i.e. represent partial derivatives with respect to only one state variable, as in

$$h_{ki} = \frac{\partial h_k}{\partial x_i} \tag{15}$$

By combining (13) and (14) and considering the contribution of a single measurement k, the admittances of the gain matrix can be computed through

$$\begin{cases} y_{k,i}^{SA} = \frac{h_{ki}}{\sigma_k^2} \sum\limits_{j=1}^{n} h_{kj} \\ y_{k,ij}^{BA} = -\frac{h_{ki}h_{kj}}{\sigma_k^2} \end{cases} \tag{16}$$

In this paper as in [10], it is assumed that the state vector $\boldsymbol{x}$ is composed by the set of bus voltage magnitudes of the network

$$\boldsymbol{x} = [V_1, V_2, ..., V_n]^T \tag{17}$$

Furthermore, it is assumed that network branches follow the general two-port π model with negligible shunt admittances, as in Fig. 1

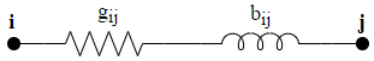

Figure 1. Two-port π model network branch with negligible shunt admittances.

where g_{ij} and b_{ij} are, respectively, the conductance and the susceptance of the network branch. Based on this assumption, the available measurements used in this paper are listed in Table I,

Table I
AVAILABLE MEASUREMENTS

Type of measurement	Expression
Real power injection at bus i, P_i	$V_i \sum_{j \in \aleph_i} V_j(G_{ij}cos\theta_{ij} + B_{ij}sin\theta_{ij})$
Reactive power injection at bus i, Q_i	$V_i \sum_{j \in \aleph_i} V_j(G_{ij}sin\theta_{ij} - B_{ij}cos\theta_{ij})$
Line current Flow magnitude from bus i to bus j, I_{ij}	$\sqrt{(g_{ij}^2 + b_{ij}^2)(V_i^2 + V_j^2 - 2V_iV_jcos\theta_{ij})}$
Voltage magnitude at bus i, V_i	V_i

where $\theta_{ij} = \theta_i - \theta_j$; $\boldsymbol{G}$ and $\boldsymbol{B}$ are in this context, respectively, the real and imaginary matrices of the admittance matrix $\boldsymbol{Y}$ and $\aleph_i$ is the set of all consecutive buses to bus i [13].

From Table I, it is possible to derive the expressions that determine the elements of the measurement Jacobian matrix $\boldsymbol{H}$. It is important to note that when considering a distribution network, $\theta_{ij} \simeq 0$. This simplification can be used to obtain the admittances of the measurements intended for allocation. However, when measurements are not being allocated as admittances, $\theta_{ij} \simeq 0$ is not considered and the formulation presented in Table I is adopted. The reasoning is to obtain the most precise solution whenever full detail is possible, specifically when using either real and reactive power injection measurements.

When considering a voltage magnitude meter at bus i, $h_k = x_i = V_i$. Based on that and according to (15)

$$\begin{cases} h_{ki} = \frac{\partial h_k}{\partial x_i} = \frac{\partial V_i}{\partial V_i} = 1 \\ h_{kj} = \frac{\partial h_k}{\partial x_j} = \frac{\partial V_i}{\partial V_j} = 0 \end{cases} \tag{18}$$

Following that, from (16) comes that

$$\begin{cases} y_{k,i}^{SA} = \frac{1}{\sigma_k^2} \\ y_{k,ij}^{BA} = 0 \end{cases} \tag{19}$$

As a result, when a meter of this type is allocated at bus i, the only resulting admittance is a shunt admittance, i.e. an admittance which connects bus i to the ground. It is also important to point out that its value only depends on the accuracy of the meter, through σ_k^2. Furthermore, the associated position of the admittance is represented by $\boldsymbol{M}_k$, which is a zero vector, except on the index of the bus where the meter is placed, which has the value 1.

On the contrary, when considering a current magnitude meter between two consecutive buses i and j and a non-consecutive bus l comes that

$$\begin{cases} h_{ki} = \frac{\partial I_{ij}}{\partial V_i} = \sqrt{g_{ij}^2 + b_{ij}^2} \\ h_{kj} = \frac{\partial I_{ij}}{\partial V_j} = -\sqrt{g_{ij}^2 + b_{ij}^2} \\ h_{kl} = \frac{\partial I_{ij}}{\partial V_l} = 0 \end{cases} \tag{20}$$

and consequently

$$\begin{cases} y_{k,i}^{SA} = 0 \\ y_{k,ij}^{BA} = \frac{g_{ij}^2 + b_{ij}^2}{\sigma_k^2} \\ y_{k,il}^{BA} = y_{k,jl}^{BA} = 0 \end{cases} \tag{21}$$

In this case, the resulting admittance is not a shunt admittance but instead a branch admittance. Moreover, its value does not only depend on the accuracy of the measurement placed but also on the values of the parameters of the corresponding branch. The associated position of the admittance comes from $\boldsymbol{M}_k$, which is a zero vector except on the indices of the buses that connect the branch where the meter is placed. In this vector, one of these indices has the value 1 and the other the value -1.

It is also worth mentioning the elements of $\boldsymbol{H}$ related with the real power injections

$$\begin{cases} h_{ki} = \frac{\partial P_i}{\partial V_i} = 2V_iG_{ii} + \sum_{j \in \aleph_i} V_j(G_{ij}cos\theta_{ij} + B_{ij}sin\theta_{ij}) \\ h_{kj} = \frac{\partial P_i}{\partial V_j} = V_i(G_{ij}cos\theta_{ij} + B_{ij}sin\theta_{ij}) \end{cases} \tag{22}$$

and reactive power injections

$$\begin{cases} h_{ki} = \frac{\partial Q_i}{\partial V_i} = -2V_iB_{ii} + \sum_{j \in \aleph_i} V_j(G_{ij}sin\theta_{ij} - B_{ij}cos\theta_{ij}) \\ h_{kj} = \frac{\partial Q_i}{\partial V_j} = V_i(G_{ij}sin\theta_{ij} - B_{ij}cos\theta_{ij}) \end{cases} \tag{23}$$

as they comprise the set of pseudo-measurements available in this study.

C. MILP Formulation

The objective of this optimal meter placement method is to find the optimal location for meters in order to minimize the SE standard error at each bus. This information can be understood to be in the diagonal elements of the covariance matrix of the state estimate. Consequently, the performance

index, which shall be referred to as error index, can be expressed as a linear combination of the diagonal elements of $\boldsymbol{R}_{\hat{\boldsymbol{x}}}$. However, this matrix only refers to the SE accuracy obtained under one load level. If one is to consider multiple load levels and wishes to get a meter configuration that obtains the best SE accuracy when applied to all scenarios considered, it is necessary to consider all the corresponding $\boldsymbol{R}_{\hat{\boldsymbol{x}}}$ matrices. Accordingly, the error index can be formulated as

$$\min \sum_{i=1}^{nN_s} \varepsilon_{ii} \tag{24}$$

where N_s corresponds to the number of scenarios considered. Each of these scenarios corresponds to the set of power measurements obtained at each bus under a determined time interval. Fig. 2 illustrates a possible procedure for generating scenarios from a set of n bus load profiles by sampling in time.

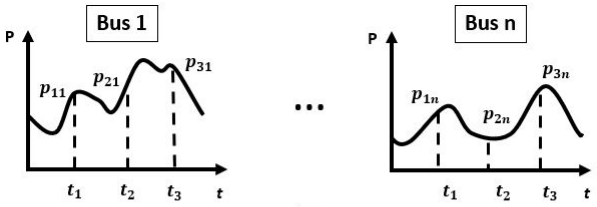

Scenario	Bus 1	Bus 2	...	Bus n
1	p_{11}	p_{12}	...	p_{1n}
2	p_{21}	p_{22}	...	p_{2n}
3	p_{31}	p_{32}	...	p_{3n}

Figure 2. Illustration of a possible procedure for generating scenarios from a set of n bus load and DER profiles. Each scenario is generated by selecting the active power measurement of each bus in a given time instant.

With sampling, one can accurately represent uncertainty without weighting the likelihood of scenarios. For other possible approaches to scenario generation, when weighting is required, the summation in (24) may be changed into a weighted sum of errors.

The elements of each covariance matrix of the state estimate can be obtained through (10). However, this operation is non-linear and threatens the formulation of the problem in a MILP format. The solution to this issue comes from decomposing the gain matrix into two parts

$$\boldsymbol{G} = \boldsymbol{G}_0 + \sum_{k=1}^{N_{cand}} \boldsymbol{M}_k b_k y_k \boldsymbol{M}_k^T \tag{25}$$

The first part, $\boldsymbol{G}_0$, corresponds to the gain matrix obtained from the initial configuration of measurements already allocated in the network. The second represents a summation of gain matrices. Each gain matrix is computed based on the allocation, in the network, of only one of the total amount of meters that can be allocated, N_{cand}. This second part is formulated similarly to (14). The sole difference is the introduction of the decision variable b_k. This decision variable refers to the allocation or not of meter k. Since the meters that are to be allocated are voltage magnitude meters and current magnitude meters, the decision vector $\boldsymbol{b}$ can be separated into two

$$\boldsymbol{b} = [\boldsymbol{b}^{vol} \;\; \boldsymbol{b}^{cur}]^T \tag{26}$$

These vectors $\boldsymbol{b}^{vol}$ and $\boldsymbol{b}^{cur}$ store the decision of allocation, $b_k = 1$, or not, $b_k = 0$ for each meter. In the case of voltage meters at each bus, while in the case of current meters at each branch. From the decomposition of the gain matrix it is possible to combine both (10) and (25) into one

$$\boldsymbol{G}_0 \boldsymbol{R}_{\hat{x}} + \sum_{k=1}^{Ncand} \boldsymbol{M}_k b_k y_k \boldsymbol{M}_k^T \boldsymbol{R}_{\hat{x}} = \boldsymbol{I} \tag{27}$$

At this point, (27) is nonlinear, and it is still not possible to formulate the optimal meter placement problem as a MILP. However, it is possible to define an instrumental vector $\boldsymbol{z}_k$ to deal with the nonlinear nature of the equation

$$\boldsymbol{z}_k = b_k y_k \boldsymbol{M}_k^T \boldsymbol{R}_{\hat{x}} \;,\; k = 1, 2, \ldots m \tag{28}$$

The purpose of this vector is to select the nonlinear part of the equation in order to apply the disjunctive model proposed by Bahiense et al. [16]. According to this model, the multiplication of decision variables in (28) disappears, and this equation is replaced by a linear relaxation

$$-L(1 - b_k)\mathbf{1} \leq \boldsymbol{z}_k - y_k \boldsymbol{M}_k^T \boldsymbol{R}_{\hat{x}} \leq L(1 - b_k)\mathbf{1} \tag{29}$$

where L is a large number and $\mathbf{1} = [1\ 1\ \ldots\ 1]$. Nevertheless, this inequality does not ensure that when $b_k = 0$, the resulting gain matrix associated with measurement k is a zero matrix. For this reason, another inequality is needed

$$-Lb_k\mathbf{1} \leq \boldsymbol{z}_k \leq Lb_k\mathbf{1} \tag{30}$$

The joint effort of both (29) and (30) leads to the intended result without any nonlinearities involved. When there is no allocation $b_k = 0$, and consequently $\boldsymbol{z}_k = \mathbf{0}$. On the contrary, when there is allocation $b_k = 1$ and $\boldsymbol{z}_k = y_k \boldsymbol{M}_k^T \boldsymbol{R}_{\hat{x}}$.

This formulation also takes into account the maximum amount of meters intended to employ with two new constraints that can be added to the problem

$$\sum_{i=1}^{n} b_i^{vol} \leq N_{new}^{vol} \;,\; \sum_{i=1}^{N_b} b_i^{cur} \leq N_{new}^{cur} \tag{31}$$

where N_{new}^{vol} and N_{new}^{cur} are, respectively, the maximum amount of voltage and current magnitude meters that can be allocated.

Additionally, a cost can be associated with each meter allocation

$$\boldsymbol{C}^T \boldsymbol{b} \leq c_{total} \tag{32}$$

where $\boldsymbol{C}$ is a vector with the costs of allocating each meter and c_{total} is the maximum amount to spend in the allocation of meters.

A new constraint is also introduced such that it is possible to define the initial position of the meters intended to allocate

$$\boldsymbol{A}^T\boldsymbol{b} = a_{total} \tag{33}$$

where $\boldsymbol{A}$ is a zero vector filled with ones in the positions where the meters are to be allocated. Accordingly, a_{total} is the result of the sum of the elements of $\boldsymbol{A}$.

The final MILP formulation can be expressed as

$$\begin{aligned}
\text{minimize} \quad & \sum_{i=1}^{nN_s} \varepsilon_{ii} \\
\text{subject to} \quad & \boldsymbol{G}_{0_1}\boldsymbol{R}_{\hat{x}_1} + \sum_{k=1}^{Ncand} \boldsymbol{M}_k b_k y_k \boldsymbol{M}_k^T \boldsymbol{R}_{\hat{x}_1} = \boldsymbol{I} \\
& -L(1-b_k)\mathbf{1} \leq \boldsymbol{z}_k - y_k \boldsymbol{M}_k^T \boldsymbol{R}_{\hat{x}_1} \leq L(1-b_k)\mathbf{1} \\
& \vdots \\
& \boldsymbol{G}_{0_{N_s}}\boldsymbol{R}_{\hat{x}_{N_s}} + \sum_{k=1}^{Ncand} \boldsymbol{M}_k b_k y_k \boldsymbol{M}_k^T \boldsymbol{R}_{\hat{x}_{N_s}} = \boldsymbol{I} \\
& -L(1-b_k)\mathbf{1} \leq \boldsymbol{z}_k - y_k \boldsymbol{M}_k^T \boldsymbol{R}_{\hat{x}_{N_s}} \leq L(1-b_k)\mathbf{1} \\
& -Lb_k\mathbf{1} \leq \boldsymbol{z}_k \leq Lb_k\mathbf{1} \\
& \sum_{i=1}^{n} b_i^{vol} \leq N_{new}^{vol} \\
& \sum_{i=1}^{N_b} b_i^{cur} \leq N_{new}^{cur} \\
& \boldsymbol{C}^T\boldsymbol{b} \leq c_{total} \\
& \boldsymbol{A}^T\boldsymbol{b} = a_{total}
\end{aligned} \tag{34}$$

The final decision variables are the elements of all matrices $\boldsymbol{R}_{\hat{x}}$, the elements of the instrumental vectors $\boldsymbol{z}_k$ and the elements of $\boldsymbol{b}$.

This formulation allows obtaining meter placement solutions that take into account not only one scenario but N_s, extending the MILP formulation presented by Chen et al. [10]. By allowing the use of N_s scenarios instead of one, it is now possible to obtain a compromise meter placement solution that is capable of dealing with load and DER volatility. This solution is defined as a compromise solution, as it may not be the optimal meter solution for every single or even any scenario individually, but instead for the whole set of possible scenarios considered.

III. Case Study

The case study presented in this paper is a radial 9 bus test feeder. The line model follows the same structure as presented in Fig. 1 and the branch admittance is $0.01 + j0.01$ p.u. It is also considered that all feeder buses, except the first, have active and reactive power injections. The measurements associated with these power injections are considered to be pseudo-measurements with 50% standard deviation. Furthermore, it is already placed a current magnitude meter between buses 1 and 2 with 1% standard deviation.

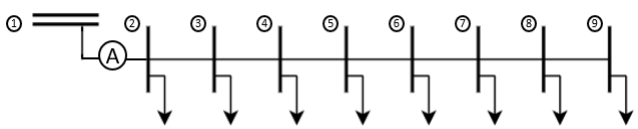

Figure 3. Nine bus test feeder.

In this paper three distinct loading situations are addressed. The first situation comprises two distinct scenarios that differ in the presence of DER. The first scenario describes a scenario without the presence of DER, in which all buses with loads have injected power equal to $-0.22 - j0.022$ p.u.. On the contrary, the second scenario describes a situation with the presence of DER, where the sole difference is the injected power at the fifth bus, which is equal to $0.88 + j0.088$ p.u..

The remaining situations are composed of twenty four scenarios and intend to reflect an evolution in the integration of DER. The second situation represents the current reality of distribution networks where there is still low DER integration, and consequently, there is low load and DER volatility. This situation compresses ninety six individual meter readings of real and reactive power injections from a single day for each bus into twenty four scenarios. This compression uses the average of each four meter readings to scale down the number of scenarios. In this situation only bus 5 has DER. For this bus, the reactive power is assumed to be 10% of the corresponding active power. The third situation assumes that all buses, except the first, can have allocated DER. Consequently, the volatility associated with this situation is higher than in the previous. In this case, real power injections at each node follow a uniform distribution with bounds $-$ 1 p.u. and 1 p.u.. The reactive power values are assumed to be 10% of the values obtained for the real power.

The aim of the tests performed is to assess the advantages of the use of a compromise meter configuration in comparison with the optimal meter configurations of each individual scenario. Tests comprise the allocation of one voltage magnitude meter and one current magnitude meter, both with 1% standard error, to both individual scenarios and the whole set of scenarios of each situation. The allocation cost at any bus or branch is considered to be the same. These meters are allocated according to the solution obtained from the MILP formulation (34) using MATLAB's Optimization Toolbox.

IV. Results and Discussion

A. Situation with Two Distinct Scenarios

Regarding the scenario without the presence of DER, the meter placement solution is presented in Fig. 4.

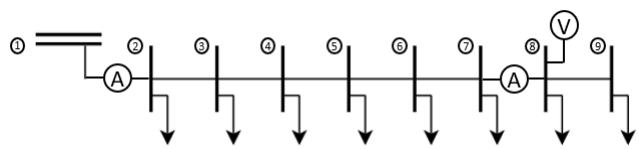

Figure 4. Optimal meter configuration considering the scenario without DER.

Besides the current magnitude meter already in place, there was the allocation of a voltage magnitude meter at bus 8 and a current magnitude meter between buses 7 and 8. The error index obtained for this meter configuration is 0.0009 p.u.

On the contrary, in regard to the scenario where there is the presence of DER, the meter placement solution is presented in Fig. 5.

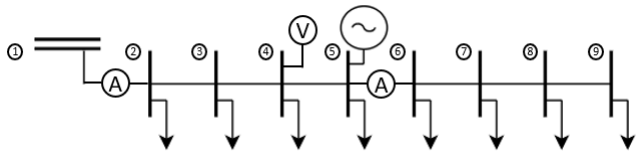

Figure 5. Optimal meter configuration considering the scenario with DER.

In this case, a voltage magnitude meter was added in bus 4, and a current magnitude meter was placed between buses 5 and 6. The error index obtained for this meter configuration is 0.0018 p.u.

The optimal meter configuration that takes into account both scenarios with and without DER is presented in Fig. 6

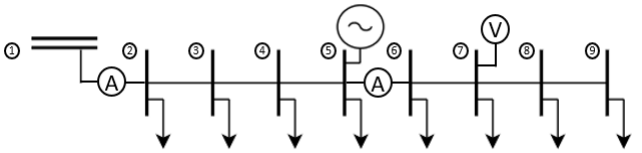

Figure 6. Optimal meter configuration considering both scenarios with and without DER.

where the voltage magnitude meter was allocated at bus 7, and the current magnitude meter was placed between buses 5 and 6.

The optimality that was previously ensured for the meter configurations that dealt with one scenario only is now also ensured by the compromise meter solution, as presented in Fig. 7.

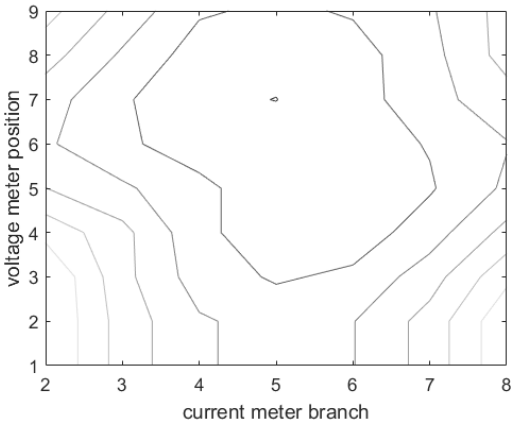

Figure 7. Contour plot of the error index considering both scenarios with and without DER. The best possible configuration that considers both scenarios has a voltage meter at bus 7 and a current meter at branch 5. This branch corresponds to the branch between buses 5 and 6.

The result obtained and presented in Fig. 7 sustains the fact that the compromise meter solution remains as its counterparts a globally optimal solution.

After obtaining the three optimal meter configurations, each configuration was assessed under each scenario individually. The resulting error indices are presented in Table II.

Table II
ERROR INDEX COMPARISON BETWEEN EACH CONFIGURATION

		Scenario Error Index (pu)	
		Without DER	With DER
Configurations	Without DER (Fig. 4)	0.0009	0.0037
	With DER (Fig. 5)	0.0015	0.0018
	Compromise (Fig. 6)	0.0011	0.0019

As anticipated and according to Table II, the configuration that has the lowest error index for a determined scenario is the configuration specifically designed for that scenario. In both scenarios, the remaining configurations present a worse error index and, consequently, a worse SE accuracy. However, the results obtained with the compromise meter solution stand out in each scenario, specifically when comparing to the other configuration that was not designed for the scenario considered. In fact, the increase in the error index is significantly lower when using the compromise meter solution rather than when using the configuration that was not designed for that scenario. This is an important result, as this is verified not only on the scenario without DER but also on the scenario with DER. Thus, these results support the use of a compromise meter solution when dealing with load and DER volatility as it can be further verified through Fig. 8.

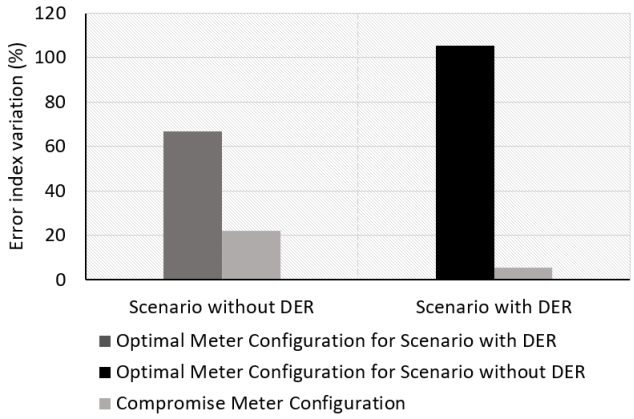

Figure 8. Comparison between error index variations obtained for different optimal meter solutions. Error variations are referred to the error index found for the optimal meter configuration of each scenario.

Further analysis on the effectiveness of the choice of the compromise solution can be obtained through the comparison of the SE standard error at each bus. This comparison for the scenario without DER is presented in Fig. 9.

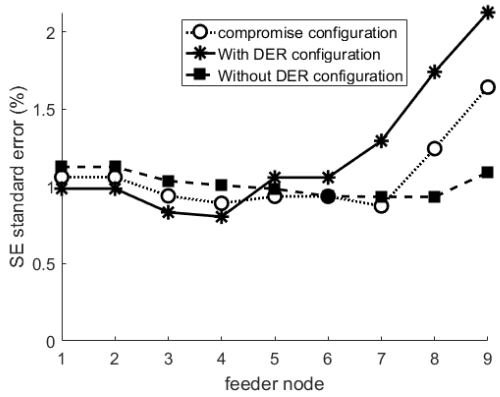

Figure 9. Comparison between the SE standard error at each bus obtained for each configuration under the scenario without DER.

From Fig. 9, some conclusions can be drawn regarding the performance comparison between meter configurations and regarding the performance of each meter configuration individually. When comparing performances between meter configurations, it is noticeable that on average, the configuration that was designed for this scenario has the best SE accuracy. On the contrary, the configuration designed for the scenario with DER has, on average, the worst SE accuracy. The SE accuracy of the compromise solution tends to stay in between the two other configurations, as intended. It is also important to notice that these conclusions are for the average and not for the individual SE of each bus. In fact, in some cases such as when considering bus 4, the configuration for the scenario with DER has a better SE accuracy than the configuration without DER. This happens because in the configuration with DER there is a voltage magnitude meter placed at bus 4 and the meters used are allocated until bus 6.

The comparison of the SE standard error at each bus considering the scenario with DER is presented next in Fig. 10.

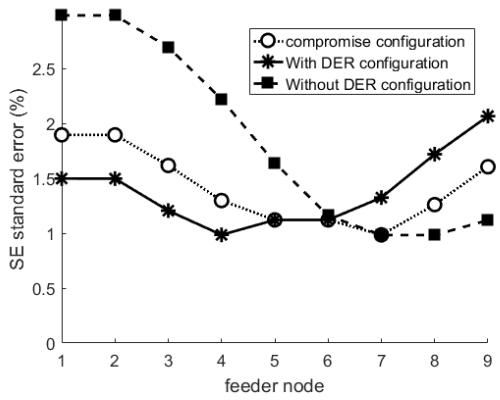

Figure 10. Comparison between the SE standard error at each bus obtained for each configuration under the scenario with DER.

From Fig. 10, it is possible to understand the reason behind the less effective performance of the configuration with DER in the previous scenario, based on the performance of the configuration without DER in this scenario. In fact, the configuration without DER has a significantly worse SE accuracy at the beginning of the feeder, as it does not take into account the effect of the presence of DER. Furthermore, as intended, the compromise solution remains with a reasonable performance.

B. Situations with Twenty Four Distinct Scenarios

The second situation represents a situation with low integration of DER, and consequently, with low net-load volatility. The compromise meter configuration for the twenty four scenarios considered is presented in Fig. 11.

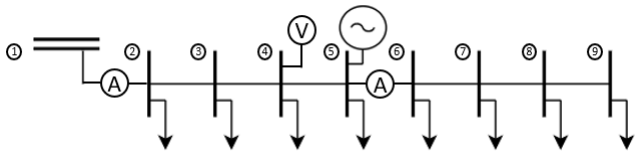

Figure 11. Compromise optimal meter configuration. The set of scenarios considered is from the second situation.

Optimal meter configurations were also obtained for each of the twenty four individual scenarios. From the set of configurations obtained, there were only two distinct solutions. One of these configurations not only was equal to the compromise solution but was also chosen by the largest amount of scenarios, about 54%, as their optimal meter configuration. Following this, configurations are compared based on their performance when applied to the whole set of scenarios as presented in Fig. 12.

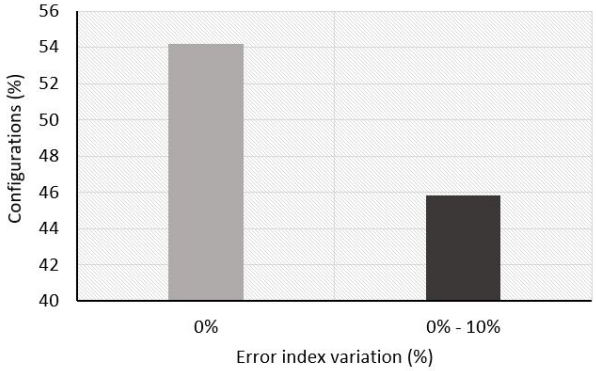

Figure 12. Comparison of the error index variation between twenty four meter configurations when each configuration is applied to the whole set of scenarios of the second situation. Error index variations are referred to the error index found for the compromise meter solution.

In this situation, it is shown that the impact of preferring the use of a compromise meter solution rather than an individual optimal solution is small. The reason for this low increase in the error index variation is that in this situation, there is low load and DER volatility at each bus. This low volatility, in turn, translates into a situation where there is low diversity in the choice of optimal meter configurations for each scenario and the impact of choosing distinct individual optimal configurations is not significant.

The previous situation can be further extended considering that all buses, except the first, can have DER. The immediate result is a substantial increase in load and DER volatility of the network. The compromise solution for the whole set of scenarios is presented in Fig. 13.

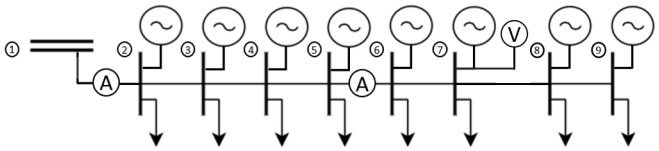

Figure 13. Compromise optimal meter configuration. The set of scenarios considered is from the third situation.

From these scenarios, eleven distinct configurations were found. One of these configurations corresponds to the compromise meter configuration, which, in this case, was only chosen by about 8% of the scenarios as their optimal meter configuration. The corresponding comparison of performance between meter configurations when applied to the whole set of scenarios is presented in Fig. 14.

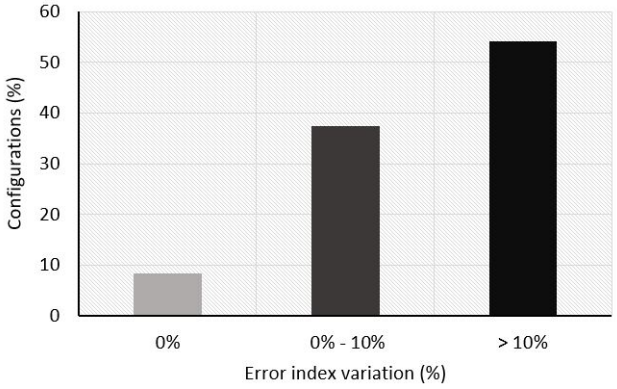

Figure 14. Comparison of the error index variation between twenty four meter configurations when each configuration is applied to the whole set of scenarios of the third situation. Error index variations are referred to the error index found for the compromise meter solution.

It is important to point out that the increased volatility in this situation had a severe impact on the increase of the error index variation of the individual meter configurations, specifically when comparing with the previous situation. This shows why is it not enough to optimally choose the optimal meter configuration for one scenario and apply to the rest, but instead it is necessary to take into account the set of scenarios in study to mitigate the impact of net-load volatility on SE accuracy.

V. Conclusion

This paper proposes a MILP approach for meter placement in low observability distribution networks. The objective of this approach is to minimize the SE standard error at all buses. For that reason, a limited amount of meters is optimally allocated in such a way that is able to mitigate the impact of net-load volatility on SE accuracy. To deal with this volatility, this approach is able to provide an optimal meter configuration based on multiple scenarios representative of different load and DER profiles. This configuration is referred as the compromise meter configuration.

The results obtained show that, if one is to consider only one scenario for obtaining the meter solution, when faced with a distinct scenario, the SE standard error can become significant. Furthermore, the results also show that a compromise meter configuration can be found to efficiently deal with scenario variations, mitigating the effects on SE accuracy of the intrinsic volatility of distribution networks loads and DER. Finally, results also indicate that compromise meter configurations will play a key role in enhancing SE accuracy of future distribution networks with high DER penetration and high net-load volatility.

References

[1] European Commission, "Energy roadmap 2050," *Luxembourg: Publications Office of the European Union*, 2012.

[2] P. Mallet, P.-O. Granstrom, P. Hallberg, G. Lorenz, and P. Mandatova, "Power to the people!: European perspectives on the future of electric distribution," *IEEE Power and Energy Magazine*, vol. 12, pp. 51–64, 2014.

[3] The European Parliament and Council of the European Union. "Directive (EU) 2018/2001 of the European Parliament and of the Council of 11 December 2018 on the promotion of the use of energy from renewable sources," 2018, http://data.europa.eu/eli/dir/2018/2001/oj.

[4] DNV GL - Energy in cooperation with Imperial College and NERA Economic Consulting, "Integration of renewable energy in europe," European Commission, Tech. Rep. 9011-700, 2014.

[5] P. M. S. Carvalho, P. F. Correia, and L. A. F. M. Ferreira, "Distributed reactive power generation control for voltage rise mitigation in distribution networks," *IEEE Transactions on Power Systems*, vol. 23, no. 2, pp. 766–772, May 2008.

[6] I. L. Roca and P. M. S. Carvalho, "Solving ill-conditioned state-estimation problems in distribution grids with Hidden-Markov Models of load dynamics," *IEEE Transactions on Power Systems*. [in press] doi: 10.1109/TPWRS.2019.2928211

[7] F. C. Schweppe and J. Wildes, "Power system static-state estimation, part I: Exact model," *IEEE Transactions on Power Apparatus and Systems*, vol. PAS-89, no. 1, pp. 120–125, Jan 1970.

[8] A. Monticelli and F. F. Wu, "Network observability: Identification of observable islands and measurement placement," *IEEE Power Engineering Review*, vol. PER-5, no. 5, pp. 32–32, May 1985.

[9] R. Singh, B. C. Pal, and R. B. Vinter, "Measurement placement in distribution system state estimation," *IEEE Transactions on Power Systems*, vol. 24, no. 2, pp. 668–675, 2009.

[10] X. Chen, J. Lin, C. Wan, Y. Song, S. You, Y. Zong, W. Guo, and Y. Li, "Optimal meter placement for distribution network state estimation: A circuit representation based MILP approach," *IEEE Transactions on Power Systems*, vol. 31, no. 6, pp. 4357–4370, 2016.

[11] J. Liu, F. Ponci, A. Monti, C. Muscas, P. A. Pegoraro, and S. Sulis, "Optimal meter placement for robust measurement systems in active distribution grids," *IEEE Transactions on Instrumentation and Measurement*, vol. 63, no. 5, pp. 1096–1105, May 2014.

[12] M. Armendariz, D. Babazadeh, L. Nordström, and M. Barchiesi, "A method to place meters in active low voltage distribution networks using BPSO algorithm," in *2016 Power Systems Computation Conference (PSCC)*, 2016, pp. 1–7.

[13] A. Abur and A. G. Exposito, *Power System State Estimation: Theory and Implementation.* CRC Press, 2004.

[14] A. Monticelli, *State Estimation in Electric Power Systems: A Generalized Approach*. Kluwer Academic Publishers, 1999.

[15] F. F. Wu, "Power system state estimation: a survey," *International Journal of Electrical Power & Energy Systems*, vol. 12 , no. 2, pp. 80–87, 1990.

[16] L. Bahiense, G. C. Oliveira, M. Pereira, and S. Granville, "A mixed integer disjunctive model for transmission network expansion," *IEEE Transactions on Power Systems*, vol. 16, no. 3, pp. 560–565, Aug 2001.